JOURNAL OF AIRCRAFT
Vol. 43, No. 4, July–August 2006

Optimization of Flexible Approach Trajectories Using a Genetic Algorithm

F. J. Vormer,* M. Mulder,† M. M. van Paassen,‡ and J. A. Mulder§
Delft University of Technology, 2600 GB Delft, The Netherlands

Current air traffic management in the terminal area is based on published sets of standard routes. However, a new procedure called the continuous descent approach has been recently proposed to decrease noise disturbances. To allow increased use of continuous descents and simultaneously increase performance in terms of other important aspects such as throughput, it may be beneficial to replace the predetermined fixed approach trajectories with more flexible trajectories instead. This is studied through optimizing approach trajectories, for which a genetic algorithm is used. Analyses show that allowing more flexibility in the approach routes can increase throughput, enable scheduling trajectories closer to continuous descent approaches, and result in routing flights less often over residential areas. However, it is also shown that flexible approach trajectories may increase airspace complexity, which in effect may make the task of air traffic control more complicated.

Nomenclature

a = longitudinal acceleration, dV_C/dt
CR_H = mean maximum horizontal closure rate
CR_V = mean maximum vertical closure rate
d = time deviation
$\hat{E}$ = energy rate demand
F = objective function value
f = fitness
h = altitude
L = noise load on community; length
M = number of segments
N = number of flights
N_8 = maximum number of aircraft pairs with less than 8-n mi (14.82 km) horizontal distance
N_{13} = maximum number of aircraft pairs with less than 13-n mi (24.08 km) horizontal distance
N_{ac} = maximum number of aircraft with an altitude change rate over 500 ft/min (2.54 m/s)
N_C = number of crossings points between arrival and departure flows
N_{pk} = peak number of aircraft simultaneously in the terminal area
N_{sc} = maximum number of aircraft with an airspeed change greater than 10 kn (5.14 m/s) during a 2-min interval
R = radius
S_H = mean minimum horizontal separation distance
S_V = mean minimum vertical separation distance
T = segment type; throughput
V_C = calibrated airspeed
V_g = ground speed
γ = flight-path angle
Δ_h = maximum deviation from altitude profile
Δ_V = maximum deviation from speed profile
ρ = aspiration level
ρ^* = constrained aspiration level
Φ = bank angle
χ = track angle

Received 16 February 2005; revision received 11 May 2005; accepted for publication 11 May 2005.

*Ph.D. Student, P.O. Box 5058, Simona International Research Institute for Simulation, Motion and Navigation, Faculty of Aerospace Engineering; currently with Preston Aviation Solutions, 488 Victoria Street, Richmond, VIC 3121 Melbourne, Australia; frizovormer@yahoo.com. Member AIAA.

†Assistant Professor, P.O. Box 5058, Control and Simulation Division, Faculty of Aerospace Engineering. Member AIAA.

‡Associate Professor, P.O. Box 5058, Control and Simulation Division, Faculty of Aerospace Engineering.

§Professor, P.O. Box 5058, Control and Simulation Division, Faculty of Aerospace Engineering. Member AIAA.

Introduction

CURRENT air traffic management (ATM) systems are based on published sets of standard arrival routes (STARs) and standard instrument departures (SIDs). These SIDs and STARs have often been designed as minimum-noise routings, but the use of new procedures such as the continuous or three-degree decelerated approach has been proposed to reduce noise impact further.[1–3] However, operational speed, altitude constraints, and ad hoc controller instructions to solve conflicts and guarantee the required throughput impede the use of these new procedures and result in more noise than theoretically necessary.[4]

A more strategic trajectory-based ATM has been proposed to reduce the need for tactical interventions. This can be achieved with the assistance of automated decision support tools, which make more reliable predictions available to air traffic controllers. In addition, most of these tools employ centralized trajectory optimization algorithms and advise controllers on actions that optimize performance, which usually refers to minimizing the amount of delays. Examples of such tools are the Amsterdam advanced air traffic control (ATC) system, the computer-oriented metering planning and advisory system, the means to aid expedition and sequencing of traffic with research of optimization system,[5] the arrival manager,[6] the center terminal radar approach control (TRACON) automation system,[7] and the tools developed within the Programme for Harmonised Air Traffic Management Research in Eurocontrol.[8] These tools typically treat trajectory optimization mathematically as solving a single-objective problem, and in case of multiple objectives, choices are made on the relative importance of these objectives before optimizing. It has been suggested, however, that a truly multi-objective scheduling process may yield better solutions in terms of supporting air traffic controllers in making choices between tradeoffs.[9]

In addition, the approach trajectories used in the mentioned tools within the terminal area are essentially STARs, where the lateral, vertical, and speed profiles were constrained due to ATC considerations. Allowing a greater degree of flexibility in the shape of the four-dimensional approach trajectory, however, may allow increased use of continuous descents and increased performance in terms of other important aspects in ATM such as runway throughput and environmental impact.[1,10,11] The tools for communication, navigation, and surveillance that enable such new trajectories are already largely

available or under development[12]: The introduction of satellite navigation has increased navigation accuracy significantly, also during the arrival procedure. Curved instead of straight-in approaches may be flown with the help of the microwave landing system. In addition, most modern aircraft are equipped with a flight management system that supports area navigation, which removes the necessity to follow ground-based navigation fixes and which is capable of predicting the flight path accurately. Data link, which is currently being introduced in practice, will allow sending much more extensive packages of data between aircraft and ground stations, including eventually the entire planned trajectory. A concern though is that greater flexibility may result in the airspace becoming less structured. This is generally referred to as an increase in airspace complexity, which may complicate the tasks of air traffic controllers.[13]

The first objective of this study is to determine if performance in terms of runway throughput, the use of continuous descents (which relates to noise production and fuel costs), and environmental impact can be increased by allowing flexible approach trajectories in the terminal area. Only arrival traffic is considered. The second objective is to determine if this results in airspace complexity becoming higher. A multi-objective trajectory optimization algorithm is used that is based on genetic optimization. The problem that this algorithm has to solve is discussed first, after which the development of the algorithm will be discussed. The study then compares the solutions that are found with this algorithm for fixed-approach trajectories with the solutions obtained for trajectories where optimization is allowed with respect to the altitude profile, speed profile, lateral profile, and location of the final interception point. The analysis is done for Amsterdam Airport Schiphol in The Netherlands as an example.

Problem Statement

Airspace Considerations

Only the terminal area of Schiphol is considered. Traffic is considered from the start of the approach until landing. The approach for Schiphol is normally started from one of the meter fixes, Artip, Sugol, or River, through which the terminal area is entered. This is usually done between about 7000 (2134 m) and 10,000 ft (3048 m). The navigation between this point and interception of final approach course is currently based on radar vectoring by ATC with the STARs as standard reference trajectories (Fig. 1a). Only the STARs between the meter fixes and the runways 18C and 27 are shown, because historical data used in this work related to these only.

Interception of the instrument landing system (ILS) glide path, which prescribes a descent angle of 3 deg, generally takes place between about 7 (12.96 km) and 10 n mi (18.52 km) from the runway threshold. Although during night hours part of the approach route may be flown as a continuous descent, high traffic loads during day times normally result in insertion of level flight segments and in interception of the final approach course in level flight. Leveling off is always conducted above 2000 ft (610 m) and in general takes place outside residential areas to minimize noise disturbance for the environment.

To accommodate departure traffic, SIDs have been defined (Fig. 1b). Because in the historical data available almost all traffic departed from runways 24 and 18L, the SIDs for these two runways only are shown. When departure and arrival flows need to cross, this is done at more or less standard points. These points are here referred to as crossing points.

Objectives

It is desired to maximize throughput, maximize the degree to which continuous descents can be applied, and minimize impact on the environment. The way of looking for solutions was brought into conformity with an approach called satisficing decision making[14] by defining an aspiration level ρ that prescribes a minimum-performance level for each of the objectives.[9]

The realized runway throughput T can be calculated from the scheduled landing times,

$$T = N(3600/\Delta T) \tag{1}$$

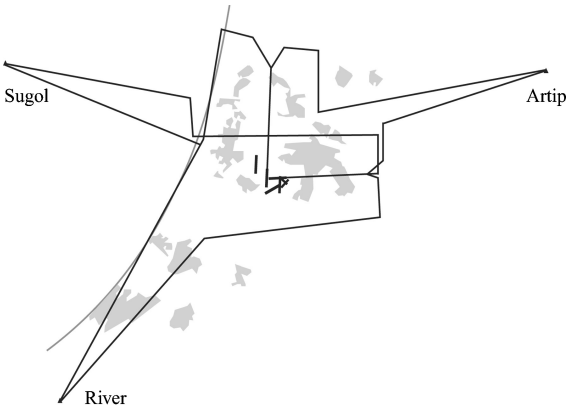

a) STARs

b) SIDs

Fig. 1 Airspace considered.

with ΔT the time interval between the first and last flight that landed. Schiphol is attempting to increase its arrival capacity to 90 movements per hour (using two arrival runways).[15] Therefore, this value is selected as the aspiration level for this objective and is denoted as ρ_T.

The deviation from a three-degree decelerated approach is taken into account by considering the maximum deviation Δ_h from a three-degree descent path and the maximum deviation Δ_V from a speed profile in such a procedure. A speed profile with a constant deceleration of 0.2 m/s^2 was considered for all traffic. Although the speed profile will be different for different aircraft in a three-degree idle descent, this deceleration is in the order of decelerations typically seen in this procedure for large aircraft. Because the goal was to obtain a first assessment of how well this type of procedure can be applied when simultaneously other objectives are optimized, this was considered a reasonable starting point. The aspiration level for Δ_h was set to 1000 ft (305 m) and is denoted as ρ_h. The reason for this was that it is the standard vertical separation distance currently applied in radar-controlled airspace. Controllers generally issue speed changes in the order of 20 (10.29 m/s)–40 kn (20.58 m/s). An aspiration level ρ_V of 20 kn was, therefore, started with.

The issue of noise production and emissions was incorporated in the objectives discussed earlier through incorporating continuous decelerated descents. It was, however, desired to determine to what degree aircraft were routed over residential areas because this is also an important part of the disturbance put on the environment. An additional measure describing noise load on community was, therefore, used, which is denoted as L,

$$L = \begin{cases} 0 & \text{if } (x, y) \notin A \\ \Delta t/h^2 & \text{if } (x, y) \in A \end{cases} \tag{2}$$

with the area A an approximation of the residential zones around the airport (where A is composed of the gray zones shown in Fig. 2),

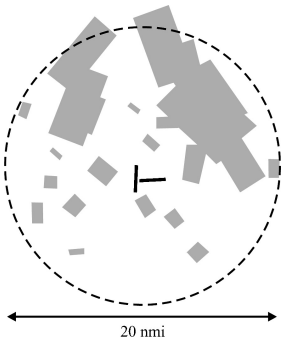

Fig. 2 Approximation of residential zones around Schiphol.

(x, y) the aircraft position in the horizontal plane, and Δt and h the time and altitude flown over A, respectively. It is unrealistic to not include altitude in this measure because traffic passing at very high altitudes will not cause disturbance. The quadratic term for altitude was used because sound intensity decreases quadratically with increasing distance between source and observer.[16] The time t was added to incorporate the effect that more time spent over an area also yields more impact on the environment. The aspiration level ρ_L is set to the value that is found for this measure for currently used approach trajectories because other reference values are not available. In this way it is required that L does not increase when flexible approach trajectories are used.

Objective Function

Because in multi-objective optimization objectives may exist that are conflicting, optimization is usually defined as looking for solutions that cannot be improved in any of the objectives without degrading the performance in at least one other objective. These solutions are called non-dominated. The collection of these solutions is referred to as the Pareto front, which contains the solutions that score mathematically equally well but that may not be equally desirable in practice.

It is possible to incorporate the score on only one objective in the objective function; this, however, does not allow finding solutions that score well on multiple objectives. It is also possible to combine the contributions from different objectives into one objective function value by using weight factors[17]; this, however, may result in solutions that score well on one objective but that have unacceptable scores on other objectives. It is not possible to obtain the set of solutions belonging to the Pareto front because the weight factors have to be chosen a priori and decision making is done before searching.[18]

To find solutions that meet all chosen aspiration levels as close as possible, the scores, on each of the objectives throughput T, altitude deviation Δ_h, speed deviation Δ_V, and noise load on community L are first normalized with respect to their aspiration levels ρ_T, ρ_h, ρ_V, and ρ_L, respectively. The objective function value F, which is to be minimized, is then taken as the maximum value of these normalized scores. The result of this is that the algorithm will try to improve the score on the objective that is least met according to the specified aspiration level, and in this way it tries to find solutions that meet all aspiration levels. Mathematically F is defined as

$$F = \max(\rho_T/T, \Delta_h/\rho_h, \Delta_V/\rho_V, L/\rho_L) \tag{3}$$

Constraints

The constraints considered are aircraft performance constraints, separation constraints, and trajectory acceptability constraints imposed by pilots and air traffic controllers.

The aircraft performance constraints consist of requiring that the calibrated airspeed should be above the minimum approach speed V_{app} and below the reference descent speed V_{des} for each aircraft. Additionally, it is required that the energy rates prescribed can be attained by the aircraft. This is done by considering the total energy E, which is composed of the potential and the kinetic energy[19] with m aircraft mass, g gravitational acceleration, h altitude, W aircraft weight, and V_g ground speed,

$$E = mgh + 1/2mV_g^2 \tag{4}$$

and the total energy rate $\dot{E}$ commanded implicitly by the reference trajectory, which is given by

$$\dot{E} = V_g W(\sin\gamma + \dot{V}_g/g) \tag{5}$$

When the equation of motion in the direction of flight is considered, the energy rate can also be written (with T thrust and D drag) as

$$\dot{E} = V_g(T - D) \tag{6}$$

The minimum energy rate that can be attained by the aircraft is approximated by using the thrust during descent T_d and the drag with speed brakes deployed $D_{\max}$,

$$\dot{E}_{\min} = V_g(T_d - D_{\max}) \tag{7}$$

To be able to compare the energy rate commanded in the trajectory with the capabilities of the subject aircraft, the ratio between the two rates is considered. This ratio is called the energy rate demand $\hat{E}$,

$$\hat{E} = \dot{E}/\dot{E}_{\min} \tag{8}$$

The energy rate demand is required to not exceed 1.

The minimum separation distances for arrival traffic are 3 n mi (5.56 km) horizontally and 1000 ft (305 m) vertically. Within the control zone, which consists of the area within 10 n mi (18.52 km) from the tower, the minimum separation is reduced to 2 n mi (3.70 km) and 400 ft (122 m). It is assumed that the two runways are operated independently. It is, therefore, considered appropriate to apply this separation only to two aircraft arriving on the same runway, provided that conventional STARs are used. On final approach the standard wake vortex separation minima depending on ICAO aircraft weight class are used.

The pilot-imposed constraints, influenced by passenger comfort considerations, prescribe a maximum bank angle of 30 deg. The minimum bank angle used is 5 deg, which is used to prevent annoyingly slow turns. The flight-path angle is limited at −6 deg because this is already considered a steep descent. Most airlines require a minimum stabilization altitude of about 500 ft (152 m), which means that at this altitude the aircraft should be stabilized and at a steady approach speed. This is incorporated by requiring a minimum stabilization distance from the runway threshold of 2 n mi (3.70 km) and a flight-path angle of −3 deg during the final approach.

Several controller-related acceptability constraints are taken into account. The airspace structure in terms of the fixed positions of the meter fixes through which arrivals enter the terminal area is not changed. Traffic was, therefore, required to enter the terminal area at a meter fix. In accordance with current practice, a maximum altitude of 10,000 ft (3048 m), a maximum calibrated airspeed of 250 kn (128.61 m/s), and a minimum altitude for leveling off of 2000 ft (610 m) were prescribed. The minimum final interception distance, the distance between the runway threshold and the point where the aircraft intercepts the ILS glide slope, was set at 3.0 n mi (5.56 km), as recommended for curved approaches.[1] Because turns longer than 180 deg would direct aircraft away from the airport, they were not allowed. To prevent routes extending to outside the terminal area, it was also required that routes are contained inside the terminal area, which was for this purpose approximated as a circle with a diameter of 70 n mi (129.64 km) around the tower.

Increasing the number of crossing points between arrival and departure traffic may well affect airspace complexity, suggesting that an upper limit is needed to keep solutions feasible and realistic with respect to air traffic control. Exactly how many additional crossing points are allowed or desired is not clear though; this is discussed further later using results from applying the optimization algorithm.

Calculating Performance

With performance, we refer to the scores that are obtained on the different objectives of throughput, altitude deviation, speed deviation, and noise load on community. If the selected aspiration levels on the objectives can be met, it would be clear that optimization can provide the desired increase in performance. However, analyses discussed later in this paper show that optimization does not allow the meeting of the aspiration levels because they are too ambitious. It

Table 1 Airspace complexity metrics

Metric no.	Metric	Notation
1	Peak number of aircraft simultaneously in the terminal area	N_{pk}
2	Maximum number of aircraft with an airspeed change greater than 10 kn during a 2-min interval	N_{sc}
3	Maximum number of aircraft pairs with less than 8-n mi horizontal distance	N_8
4	Maximum number of aircraft pairs with less than 13-n mi horizontal distance	N_{13}
5	Maximum number of aircraft with an altitude change rate over 500 ft/min	N_{ac}
6	Number of crossings points between arrival and departure flows	N_C
7	Mean minimum horizontal separation distance	S_H
8	Mean minimum vertical separation distance for traffic at less than 5-n mi horizontal proximity	S_V
9	Mean maximum horizontal closure rate	CR_H
10	Mean maximum vertical closure rate for traffic at less than 5-n mi horizontal proximity	CR_V

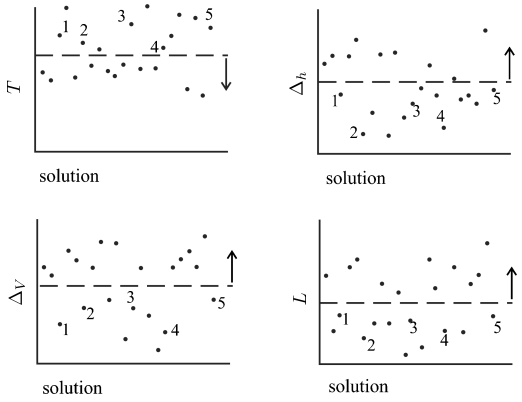

Fig. 3 Selection of constrained aspiration levels.

is, therefore, necessary to determine how the aspiration levels have to be chosen so that acceptable solutions with respect to the desired performance can be found. These levels are then a measure of the performance that can be achieved on all objectives simultaneously.

For this reason, a so-called constrained aspiration level ρ^* is established for each objective as follows. For the solutions that are found with the optimization algorithm, the scores on the objectives are assumed to be distributed normally. From all obtained values, the mean value and variation can be estimated for each objective, which makes it possible to approximate the cumulative distribution function. A level β is then selected, and each constrained aspiration level ρ^* is selected so that the fraction of solutions with more than the aspired performance according to the cumulative distribution function equals β. The initial value selected for β is 0.05, but this value is increased if necessary until five solutions (the number of solutions that was considered simultaneously) meet the constrained aspiration level ρ^* for each objective. In Fig. 3, it is shown how the aspiration levels are changed until five of the solutions found meet the constrained aspiration levels on all objectives.

Calculating Airspace Complexity

A number of metrics from literature[13] are used to accomplish the objective of assessing the effects of more flexible trajectories on airspace complexity (metrics 1–5, Table 1). The number of crossing points was added to this list because it was expected to be an important factor for airspace complexity not addressed by the other metrics. A point where arrival and departure traffic cross is only counted as a crossing point if the crossing takes place more than 5 n mi (9.26 km) from each previously found crossing point. This is to prevent counting a high number of crossing points when crossings take place at nearly the same point.

A number of simple metrics were also used that described the distances and closure rates of aircraft pairs because they are also considered important factors for airspace complexity not accounted for in the other metrics. For horizontal separation, at each point in time and for each aircraft the lowest separation with other traffic is first determined. The value of S_H is then taken as the mean value of this minimum separation over all traffic and over all time. The same is done for S_V except that only traffic in horizontal proximity is taken into account. A distance of less than 5 n mi was selected to define horizontal proximity. In a similar way, the mean maximum closure rates CR_H and CR_V are determined. Thus, all metrics used to describe airspace complexity refer to all traffic in the airspace considered.

Solution Methodology

Genetic Algorithms

The recent advent of the use of evolutionary optimization techniques has provided ways to overcome some of the disadvantages of classical solution methods of multi-objective problems by processing multiple tradeoffs in one optimization run. Because a number of solutions can be processed simultaneously, a priori decision making about the relative importance of objectives can be prevented and the Pareto front can be approximated. The most widely used of these algorithms, suitable for handling large and complex search spaces,[18] are genetic algorithms.

A genetic algorithm qualifies as a stochastic search method modeled on the process of natural Darwinian evolution (see Ref. 20). Possible solutions are encoded into strings of data, referred to as chromosomes. A solution described by a chromosome is called an individual. Each individual is assigned a fitness value f that determines its chance of survival.

The genetic algorithm starts by generating a set of individuals called an initial population. These individuals can be either randomly selected individuals or individuals that are expected to be desirable based on knowledge about the system. During the process of genetic optimization, a new population is created over and over again. These new populations are created by applying genetic operators on the existing individuals in the population. Well-known genetic operators are selection and crossover, which preserve knowledge about good solutions, and mutation, which explores new areas of the solution space.

The selection operator reproduces more copies of individuals with high-fitness values. The crossover operator creates two new individuals from two original individuals that were selected from the current population by the selection operator (Fig. 4). The original chromosomes are cut at either one or two points, and the separate pieces of genetic information are swapped and connected again, forming two new individuals. When using only the crossover operator to preserve knowledge in the population on good properties of the solutions, only different combinations of those properties are explored, and the diversity of the population will generally decrease. For this reason, a mutation operator is also applied. It changes randomly one or more values in the chromosome (Fig. 5) with a certain mutation probability. In this way, new genetic information is added to the population, which promotes new search directions and helps to avoid premature convergence.

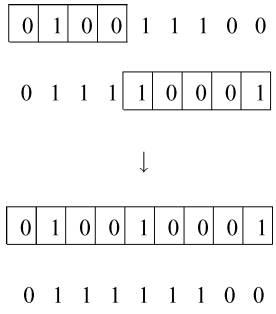

Fig. 4 One-point crossover for two individuals containing binary data.

Although chromosomes may be chosen within certain limits to satisfy constraints, for most problems it cannot be prevented that the solution proposed by the genetic algorithm violates one or more constraints. When these solutions are simply destroyed, the genetic solution search process will not be very efficient. For this reason, domain-specific strategies are often used that apply deterministic rules to proposal solutions to overcome the constraint violation. These strategies are called repairing strategies.[20]

Trajectory Definition

Several earlier studies addressed the use of genetic algorithms for route planning in ATM. Both the approach of chromosomes containing coordinates of waypoints[21–23] and containing trajectory descriptions such as segments and routes[24–26] have been applied successfully.

In this work, flight paths are represented as sets of straight and curved trajectory segments. The main reason for this is that humans generally also process trajectories in terms of segments.[27] This approach was also taken in other applications.[28,29] Other reasons for using segments include the facts that segments are a common way of describing trajectories both in air traffic control and in the flight management system and that an efficient communication or negotiation process between controllers and pilots can be supported.

The parameters to describe a segment j for a flight i are chosen as

$$\begin{gathered}\text{Segment type } T_{i,j}\\ \text{Radius } R_{i,j}\\ \text{Length } L_{i,j}\\ \text{Absolute flight-path angle } |\gamma_{i,j}|\\ \text{Absolute acceleration } |a_{i,j}|\end{gathered} \tag{9}$$

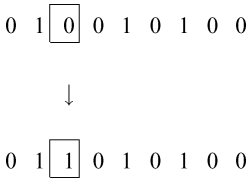

Fig. 5 Mutation for an individual containing binary data.

A straight segment is denoted as a segment of type 1, whereas types 2 and 3 are used to describe segments with left and right turns, respectively. Acceleration a is defined as the time derivative of V_C because unaccelerated flight refers in practice to constant V_C.

The reason for using the absolute signs was related to the possibility of including departure traffic and optimizing departure and arrival flights simultaneously. This coding is advantageous when a genetic algorithm is applied because an arrival trajectory can be changed to a departure trajectory without the need to change the segment's parameters. If the absolute signs are not used, additional repairing strategies will be necessary which may deteriorate the algorithm's efficiency.

To determine the entire four-dimensional trajectory, each set of segments for a flight i is extended with the following parameters:

$$\begin{gathered}\text{Flight identification code ID}_i\\ \text{Runway assignment RA}_i\\ \text{Arrival time deviation } d_i\end{gathered} \tag{10}$$

The genetic algorithm can change the scheduled time of arrival (STA) at the runway STA_i by changing the deviation d_i with respect to a nominal time of arrival NTA_i:

$$\text{STA}_i = \text{NTA}_i + d_i \tag{11}$$

The form of a gene giving a trajectory description for one flight is indicated in Fig. 6, with M the number of segments. Genes are combined into a chromosome as shown in Fig. 7, with N the number of flights.

Inputs and Outputs

The inputs to the optimization problem that the genetic algorithm is looking for are the four-dimensional trajectories for all flights. These are described with the parameters contained in the chromosome (Fig. 7): the flight identification codes $\text{ID}_{1,\ldots,N}$, runway assignments $\text{RA}_{i,\ldots,N}$, arrival time deviations $d_{i,\ldots,N}$ segment types $T_{1,\ldots,N,1,\ldots,M}$, radii $R_{1,\ldots,N,1,\ldots,M}$, lengths $L_{1,\ldots,N,1,\ldots,M}$, flight-path angles $\gamma_{1,\ldots,N,1,\ldots,M}$, and accelerations $a_{1,\ldots,N,1,\ldots,M}$. The outputs, which determine the quality of the solution, are the scores on the objectives: the throughput T, maximum deviation Δ_h from a three-degree descent path, maximum speed deviation Δ_V from a continuously decreasing speed profile, and noise load on community L.

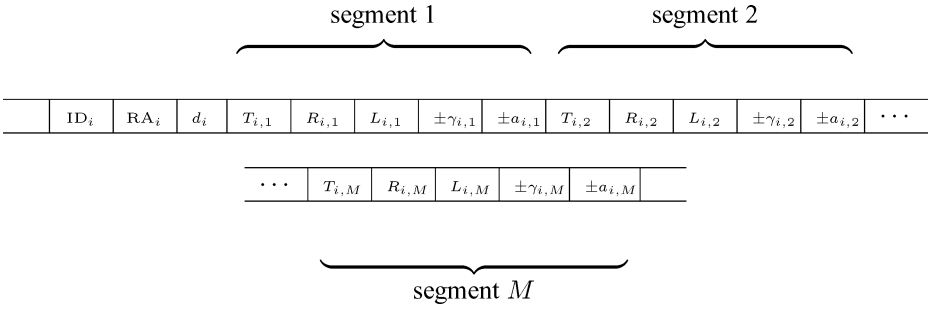

Fig. 6 Gene.

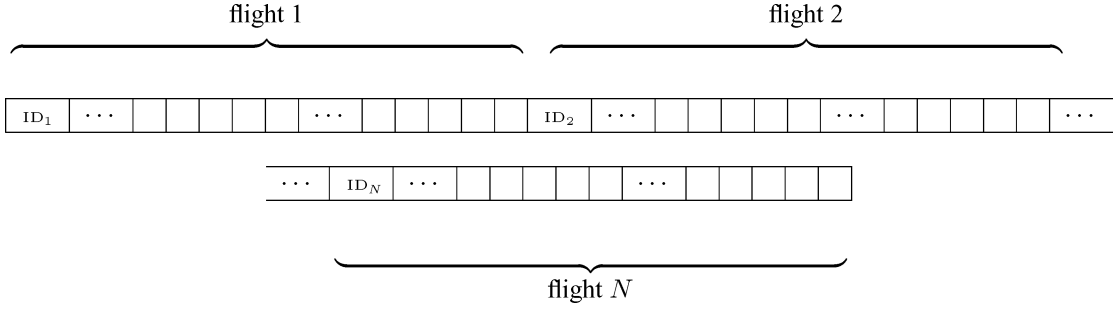

Fig. 7 Chromosome.

Table 2 Constraints

Constraint	Repairing strategy
$T \in [1, 2, 3], a \leq 0$	
$V_C \leq \min(V_{\text{des}}, 250 \text{ kn})$	Set a so that maximum speed is not exceeded
$\hat{E} \leq 1$	If $a < 0$, increase a with 0.02 m/s^2 If $a = 0$, increase γ with 0.25 deg
$\left\|\sqrt{(x_i - x_n)^2 + (y_i - y_n)^2}\right\| \geq 3$ n mi $\vee \, \|h_i - h_n\| \geq 1000$ ft $\forall i \neq n$ if $\left\|\sqrt{x_i^2 + y_i^2}\right\| \geq 10$ n mi $\vee \left\|\sqrt{x_n^2 + y_n^2}\right\| \geq 10$ n mi	Increase STA of trailing aircraft with 5 s
Conventional STARs $\left\|\sqrt{(x_i - x_n)^2 + (y_i - y_n)^2}\right\| \geq 2$ n mi $\vee \, \|h_i - h_n\| \geq 400$ ft $\forall i \neq n$ if $\left\|\sqrt{x_i^2 + y_i^2}\right\| < 10$ n mi and $\left\|\sqrt{x_n^2 + y_n^2}\right\| < 10$ n mi and $\text{RA}_i = \text{RA}_n$	
No conventional STARs $\left\|\sqrt{(x_i - x_n)^2 + (y_i - y_n)^2}\right\| \geq 2$ n mi $\vee \, \|h_i - h_n\| \geq 400$ ft $\forall i \neq n$ if $\left\|\sqrt{x_i^2 + y_i^2}\right\| < 10$ n mi and $\left\|\sqrt{x_n^2 + y_n^2}\right\| < 10$ n mi $\text{STA}_i \geq \text{STA}_n + \Delta T_{\text{sep}}(WC_i, WC_n) \vee$ $\text{STA}_i \leq \text{STA}_n - \Delta T_{\text{sep}}(WC_i, WC_n) \; \forall i \neq n$	
$5 \leq \Phi \leq 30$ deg $-6 \leq \gamma \leq 0$ deg	Set R so that bank angle limits are not exceeded
First segment from runway: $T = 1$, $L = 2$ n mi, $\gamma = -3$ deg, $a = 0$ $x_{\text{final}} = x_{\text{td}}$, $y_{\text{final}} = y_{\text{td}}$, $h_{\text{final}} = 0$, $\chi_{\text{final}} = \chi_{\text{td}}$, $V_{C,\text{final}} = V_{\text{app}}$ $\left\|\sqrt{(x_{\text{entry}} - x_{\text{mf}})^2 + (y_{\text{entry}} - y_{\text{mf}})^2}\right\| \leq 2$ n mi	Connect meter fix with first 5 segments from runway
$h \leq 10,000$ ft $\gamma \leq -3$ deg if $h < 2000$ ft	$\gamma = 0$ $\gamma = -3$ deg
Second segment from runway: $L \geq 1$ n mi $L \cos\gamma / R \leq 180$ deg $\left\|\sqrt{x^2 + y^2}\right\| \leq 35$ n mi	Set segment type to straight ($T = 1$)
$N_C \leq 11$	Use same route for more aircraft

Meeting the Objectives and Constraints

When the genetic algorithm has generated a set of chromosomes, trajectory profiles can be generated for all aircraft. This is necessary to calculate the scores on the objectives and to determine if constraints are met. For each trajectory, a four-dimensional profile is, therefore, generated by calculating aircraft states along the trajectory. The following aircraft states are calculated: horizontal position x and y (with the origin of the axis system at the location of the tower), altitude h, track angle χ, flight-path angle γ, bank angle Φ, calibrated airspeed V_C, and ground speed V_g. The time step was tuned to 2 s.

The constraints are expressed mathematically in Table 2, where both $i = 1, \ldots, N$ and $n = 1, \ldots, N$ refer to the arriving flights. In Table 2, ΔT_{sep} is the required time separation on final approach between two aircraft with weight classes WC_i and WC_n (Ref. 30), subscript td refers to the prescribed touchdown point (300 m from the threshold of the runway used), subscript final to the actual touch down point, subscript entry to the entry point into the terminal area, and subscript mf to the meter fix that is used. The constraints related to the touchdown point are met by starting the generation of the profiles from $x_{\text{final}} = x_{\text{td}}$, $y_{\text{final}} = y_{\text{td}}$, $h_{\text{final}} = 0$, $\chi_{\text{final}} = \chi_{\text{td}}$, and $V_{C,\text{final}} = V_{\text{app}}$.

The constraints that apply to parameters contained in the chromosome are applied directly by limiting these parameters to the range allowed. The constraints that apply to parameters not contained in the chromosome, however, require repairing strategies. These are also summarized in Table 2 where applicable. The values involved in the repairing strategies are very problem dependent and have been found to function well for this application. For calculation of aircraft performance parameters, the data from the Eurocontrol Base of Aircraft Data (BADA)[31] is used.

The constraint on meeting the prescribed meter fix position is met by connecting the first five segments from the runway to the meter fix. This is done by adding to these segments one curved segment and three straight segments that result in reaching the meter fix. Three straight segments were used instead of one to prevent that one segment being much larger than the others.

The number of crossing points allowed has so far not been specified. In simulations carried out in this work that modeled current operational practice, the number of crossing points was generally found to be about four. On the other hand, most of the initial solutions generated with the genetic algorithm for a system where the STAR structure was not in place had a minimum of 11 crossing points. Because this is already a large number compared to the four crossing points for current practice, it was used as an upper limit. In case candidate solutions were found with a higher number of crossings than allowed, the arrival trajectory that caused the violation was removed and replaced by a trajectory that was already scheduled for another aircraft. In this way, two aircraft used the same trajectory and the number of crossing points was reduced.

When solutions are found, the fitness f can be calculated, which is defined as $f = 1/F$, with F from Eq. (3). The inverse of F is used because the genetic algorithm maximizes fitness, whereas F needs to be minimized.

Genetic Algorithm Parameters

Because the number of segments in the standard approach routes used at the airport considered is typically about nine, the number of segments used here was set to nine also. The initial solution was obtained by filling in random values for the inputs within the range allowed. The genetic algorithm that was applied used a standard single-point crossover operator. For mutations a modified mutation operator was used that could modify all parameters except ID. The algorithm was implemented using the GAlib genetic algorithm package, which was developed at the Massachusetts Institute of Technology.[32] The crossover probability was set to 0.7 and the mutation probability to 0.1, which are within the range of typically used values[17] and which worked well for this problem. It may, furthermore, be beneficial to replace only a part of the population each generation because a good balance between population diversity and the tendency of high-fitness individuals to survive may allow desired solutions to be found earlier.[17] In this work, in each generation 50% of the population was replaced, which was also the default value applied in the mentioned algorithm package. The number of solutions

processed simultaneously was set to five. This was based on the idea that if an air traffic controller would use a tool based on this method, five was considered a reasonable number of solutions that could also be processed simultaneously by an operator. Fitness scaling based on a technique called sigma truncation[33] was also applied because this was found to yield faster improvement of the solutions. In case that constraints were not met, a maximum of 40 attempts was made to satisfy the constraints by using repairing strategies. If after this the solution was still infeasible, it was discarded.

Analysis

Assumptions

To be able to quantify any potential benefits of flexible arrival trajectories, the first situation that has to be considered is the way approaches are currently carried out. For this reason, use is made of recorded radar data from Schiphol Airport made available by ATC The Netherlands. The data concern all flights that arrived at Schiphol Airport on one particular day (12 September 1997). The main runways used for landing in the airport configuration at that time were the two runways 18C and 27. The data concern the flights from entry into the terminal area until landing and specify for all flights the aircraft type, the runway at which the aircraft landed, the meter fix that was used, the flight level at which the meter fix was crossed, the time at which the meter fix was crossed, and the time at which the aircraft landed. From these data, a traffic sample is extracted, containing 15 flights with their landing times spanning a time interval of 15–20 min, a typical time horizon in the final phase of route planning for arrival traffic. The sample was selected for a time period when traffic demand was high and is assumed to be representative of current demand at this airport. The wind direction and speed at the time the sample was taken were 240° north and 9.7 m/s, respectively (data obtained from the Royal Netherlands Meteorological Institute), and they are assumed to be representative of the atmospheric conditions near this airport.

In the genetic algorithm, 15 flights are created. For each flight, the genetic algorithm uses the aircraft type that was recorded to determine which data to use from BADA. For each flight, (x_{mf}, y_{mf}) was set to the position of the meter fix that was recorded. The NTA for each flight is set to the landing time that was recorded. The other data were incorporated differently in different situations, as discussed in the next section.

Definition of Cases

The transition from fixed routes toward more flexible routes is studied in subsequent steps. This is done through first adding operational constraints to the constraints that were already taken into account so that a model of current operations is obtained and then removing some of the constraints. This allows to quantify the effect of each step and to determine if it is worthwhile to proceed in this direction. The different steps that are studied are optimizing the landing sequences and time schedules, optimizing the altitude and speed profiles, allowing a reduced final intercept distance, allowing direct routes from the meter fix to the final intercept point, and allowing the route structure to be optimized in terms of the lateral profiles. To this end, a number of cases are defined (Table 3).

Case CUR represents the operations as recorded. The STARs shown in Fig. 1a and standard speed profiles made available by the National Aerospace Laboratory (giving reference speeds for the points where two segments were connected) were used to define the trajectories. The altitudes at the boundary of the terminal area as they were recorded in the traffic sample were used. In the turns in the traffic pattern, the altitude was kept constant to obtain a stepwise descent with level flight segments that is characteristic for current operations. On the other segments, the flight-path angle is kept constant. This was achieved by selecting the values of T, R, L, γ, and a accordingly. In the STARs, the final interception point is not placed closer to the runway threshold than 6 n mi (11.11 km) and not further away than 11 n mi (20.37 km). In addition, for this case the RAs from the recorded data are used, thus also prescribing the values of RA. This is indicated in Table 3 as Standard because these assignments correspond to standard current operations. The genetic algorithm was allowed to schedule a deviation d of ± 0.5 min from the recorded landing times because this was the accuracy with which the times in the recorded data were logged. It was found that the same requirement for meeting the recorded meter fix time could not be met. The reason for this is that the planning algorithm starts with planning in space and time at the threshold. Any differences between the model and the real situation at the time of the measured data, for example, different atmospheric conditions or different routes used by controllers, will, thus, be noticed as deviations from the recorded meter fix times. A meter fix time deviation up to ± 5.0 min was necessary to accommodate these differences. This means that the reliability of the results decreases at farther distances from the runway.

Case CUR IDEAL considers the same situation as case CUR, but now in an idealized setting by assuming that other runway assignments and landing times that are found with the genetic algorithm to result in a better solution can also be executed during real operation. The results for flexible arrival trajectories are compared with the results for case CUR IDEAL so that a fair assessment of potential benefits is assured. Comparing with case CUR is not considered fair because case CUR may include reasons not included in the other cases for disallowing certain solutions. Because we are looking for the best solution possible, the RA and landing times (in the form of d) are optimized. The landing times were required to be within ± 2.0 min of the recorded times because larger deviations from the original times did produce mostly infeasible solutions.

Case FLX TMS is defined to assess the effects of optimizing the landing sequences and times in case CUR IDEAL without requiring a maximum deviation from the originally recorded landing times, which is indicated in Table 3 with the designation not applicable (N/A). It is still desired to use an upper limit for the deviation from the original meter fix time though because otherwise the traffic demand can become different depending on the case. The maximum delay and time advance that can be given at the meter fix were limited to 15 min because this is a typical time horizon that controllers make plannings for. In each of the following cases, a specific operational constraint is changed with respect to case FLX TMS.

Case FLX ALT/SPD is defined to assess the effects of maintaining the rigid route structure but allowing the altitudes and speeds to be optimized. Therefore, the standard altitude and speed profiles are not used for this case, and the genetic algorithm is also allowed to optimize γ and a. Changing altitude and speed profiles is addressed simultaneously because they are closely related through energy management.

Case SHORT IC is defined to assess the effects of allowing a reduction of the final intercept distance to 3 n mi from the threshold, the minimum distance mentioned earlier. Allowing such a reduction

Table 3 Definition of cases

Case	Route structure	Final intercept distance, n mi	Altitude profile	Speed profile	Runway assignment	Deviation d from recorded landing time, min
CUR	Conventional	6–11	Standard	Standard	Standard	±0.5
CUR IDEAL	Conventional	6–11	Standard	Standard	Optimized	±2.0
FLX TMS	Conventional	6–11	Standard	Standard	Optimized	N/A
FLX ALT/SPD	Conventional	6–11	Optimized	Optimized	Optimized	N/A
SHORT IC	Conventional	3–6	Standard	Standard	Optimized	N/A
DIRECT	Direct	6–11	Standard	Standard	Optimized	N/A
FLX LAT	Optimized	6–11	Optimized	Optimized	Optimized	N/A

results in not applying conventional STARs any more and a different separation constraint therefore applies (Table 2). To make the differences between a conventional final intercept and a short final intercept more distinct, the maximum allowed final interception distance was 6 n mi, which was the smallest distance allowed for a conventional intercept. This is achieved by allowing the genetic algorithm to also optimize the value of L for the second segment (within the range that assures the earlier mentioned limits on the final interception distance). Because in case SHORT IC the ILS intercept takes places closer to the threshold than in the other cases, the deceleration to approach speed takes place closer to the threshold also.

Case DIRECT is defined to assess the effects of allowing direct routes instead of STARs. For all traffic direct routes are used from the meter fix to the final approach interception point by selecting the values of T, R, L, γ, and a accordingly.

Case FLX LAT is defined to assess the effects of not limiting the routes to conventional or direct routes, but instead optimizing the route structure laterally. Also for this case, STARs are not used. Because there is no fixed route structure, the standard speed and altitude profiles, which are largely based on the horizontal shape of the routes, cannot be used. The speed and altitude profiles are, therefore, optimized. The genetic algorithm is, thus, allowed to optimize T, R, L, γ, and a.

Results

Because the genetic optimization process is a stochastic process and the outcome may, therefore, be different each time, the genetic algorithm was run 30 times for each case and the results are analyzed with a statistical analysis. For all runs, Fig. 8 shows how the fitness f changes from generation to generation for each case. Because $f < 0.5$ for all runs, it follows that $F > 2$, which means that for all runs at least one of the desired aspiration levels is not met by a factor larger than 2. Thus, either the throughput T is more than two times lower than desired, or the altitude deviation Δ_h, or the speed deviation Δ_V, or the noise load on community L is more than two times higher than desired.

Note that for the first couple of cases the genetic algorithm can only provide a limited improvement in the value of f, whereas for the higher case numbers significant improvements can be made. It can also be seen that the level of convergence is different depending on the case. Although it cannot be proven that better solutions cannot be found, the genetic search process was continued for 500 generations so that for most runs reasonable convergence was achieved.

The typical shape of obtained solutions, containing the trajectories from the meter fixes to the runways, is shown in Figs. 9–11. Figures 9–11 show for all trajectories the shape of the trajectory in the horizontal plane projected on a map of the environment. The solid trajectories are the generated arrival trajectories; the dashed trajectories are the SIDs used for this runway configuration. Additionally, for all flights, the altitude h, the speed V_C, and the bank angle Φ are plotted against the reference time t. The reference time was always the same. Figure 9 shows an example of a solution for case CUR. It can be seen that standard arrival trajectories with level flight segments are used. Figure 10 shows an example of a solution for the direct routes (case DIRECT), where it can be seen that trajectories directly from the meter fix to the interception point of the final approach course are used. Figure 11 shows an example of a solution for the routes optimized in the horizontal plane (case FLX LAT). It can be seen that more airspace is used to schedule the lateral profiles and that the altitude and speed profiles contain more variation when compared to those for the other cases because they are optimized. Examples of more solutions can be found in Ref. 34.

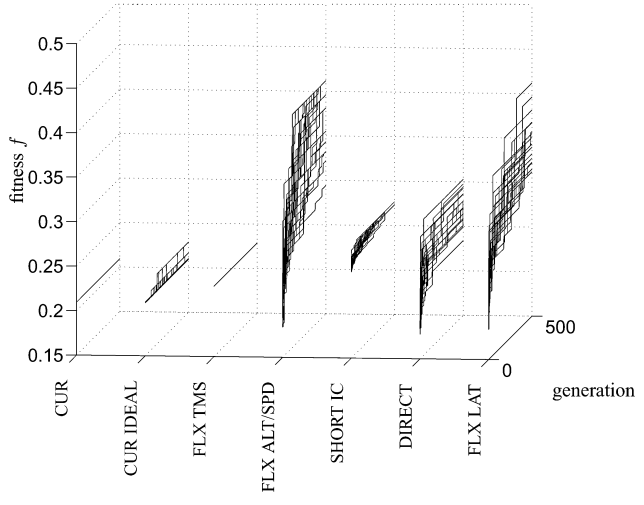

Fig. 8 Evolution of the fitness during the genetic process.

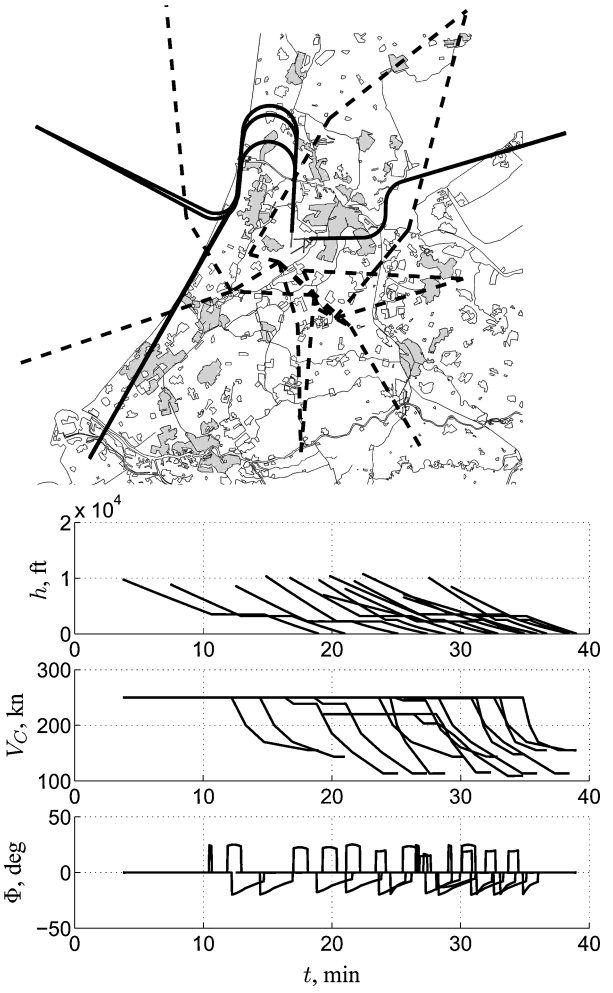

Fig. 9 Conventional routes (case CUR).

The cases are compared to each other with respect to ATM performance by comparing the scores on the objectives throughput T, altitude deviation Δ_h, speed deviation Δ_V, and noise load on community L. Because the aspiration levels are not all met, the scores are obtained by calculating the constrained aspiration levels for all objectives. The cases are compared with respect to airspace complexity by comparing the scores on the metrics N_{pk}, N_{sc}, N_8, N_{13}, N_{ac}, N_C, S_H, S_V, CR_H, and CR_V (Table 1) for the final solutions found by the genetic algorithm.

Performance

The constrained aspiration levels found are shown for the different objectives in Fig. 12, where the aspiration levels that were originally selected also are indicated. It can be concluded that the selected aspiration levels of 90 arrivals per hour for T, 1000 ft for Δ_h, and 20 kn for Δ_V are not met. This shows the difficulty of meeting all aspirations at the same time. The competitiveness of the objectives is confirmed especially by comparing cases CUR and CUR IDEAL:

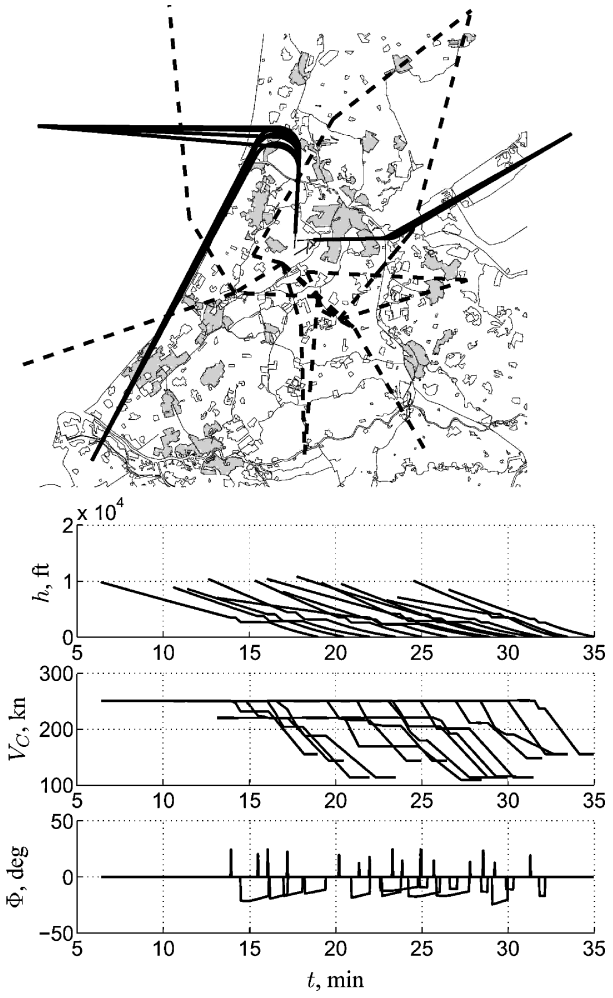

Fig. 10 Direct routes (case DIRECT).

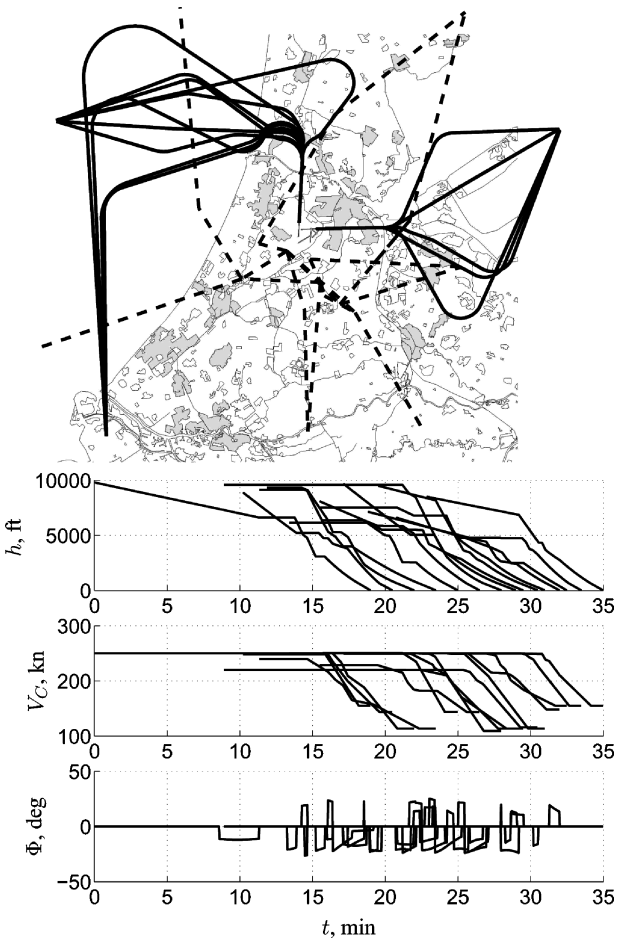

Fig. 11 Routes optimized in the horizontal plane (case FLX LAT).

Removing unmodeled influences does not increase the throughput T, which is explained by the deviation from another aspiration level being larger and more important. Statistically significant differences between the cases were, however, observed for all objectives (T: $F_{6,203} = 729.015$, $p \leq 0.01$; Δ_h: $F_{6,203} = 2350.636$, $p \leq 0.01$; Δ_V: $F_{6,203} = 1434.244$, $p \leq 0.01$; and L: $F_{6,203} = 244.615$, $p \leq 0.01$).

For the throughput T, a Student–Newman–Keuls (SNK) test with $\alpha = 0.05$ showed that cases FLX TMS, FLX ALT/SPD, SHORT IC, DIRECT, and FLX LAT resulted in higher values than case CUR IDEAL. The mean throughput was for case CUR IDEAL equal to 43.73 arrivals per hour, whereas it increased for cases DIRECT and FLX LAT to 56.16 and 56.35 arrivals per hour, respectively. This corresponds to an increase up to about 28% arrivals per hour more. Optimizing the arrival times and the trajectories is, therefore, concluded to enable increased throughput.

For the altitude deviation Δ_h, an SNK test showed that cases FLX ALT/SPD and FLX LAT (the two cases where altitude and speed profiles were optimized) are the cases with the lowest altitude deviation: The mean value of Δ_h was equal to 2560 (780 m) and 3106 ft (947 m), respectively. For case CUR IDEAL, it was equal to 4729 ft (1441 m), which confirms that optimization of the profiles resulted in altitude profiles closer to those belonging to a continuous descent approach. The reduction of the mean value for case FLX ALT/SPD as compared with case CUR IDEAL is equal to 2169 ft (661 m), which is significant because it is more than the standard vertical separation distance of 1000 ft applied by ATC.

For the speed deviation Δ_V, an SNK test showed that case SHORT IC resulted in the best score: The mean value of Δ_V was 49.08 kn (25.25 m/s), whereas for case CUR IDEAL, it was 81.43 kn (41.89 m/s). The lower deviation for case SHORT IC is explained by the later deceleration to final approach speed. The fact that lower values for Δ_V are not found for the cases where the genetic algorithm optimizes the altitude and speed profiles is explained by the fact that to resolve energy-related constraint violations the genetic algorithm favored changing the speed profile over changing the altitude profile.

For the noise load on community L, an SNK test ($\alpha = 0.05$) showed that cases CUR and CUR IDEAL resulted in the worst scores. The mean value of L was 0.00829 s/m^2 for case CUR IDEAL. The other cases all resulted in statistically significant better values for L: The lowest mean value was found for case FLX ALT/SPD and was equal to 0.00621 s/m^2, corresponding to a decrease of about 25%. This indicates that optimizing the altitude and speed profiles, allowing a short final intercept distance, applying direct routes, and optimizing the horizontal route structure all can significantly reduce the time flown over residential areas at low altitude.

Airspace Complexity

The values of the considered airspace complexity metrics are shown in Figs. 13 and 14. Statistically significant differences were found between the cases for all metrics (N_{pk}: $F_{6,203} = 15.968$, $p \leq 0.01$; N_{sc}: $F_{6,203} = 32.193$, $p \leq 0.01$; N_8: $F_{6,203} = 21.527$, $p \leq 0.01$; N_{13}: $F_{6,203} = 23.267$, $p \leq 0.01$; N_{ac}: $F_{6,203} = 42.171$, $p \leq 0.01$; N_C: $F_{6,203} = 186.460$, $p \leq 0.01$; S_H: $F_{6,203} = 108.487$, $p \leq 0.01$; S_V: $F_{6,203} = 6.918$, $p \leq 0.01$; CR_H: $F_{6,203} = 22.574$, $p \leq 0.01$; and CR_V: $F_{6,203} = 98.508$, $p \leq 0.01$).

For the peak number of aircraft in the terminal area, N_{pk}, case CUR IDEAL resulted in a mean value of 11.2. The flexible arrival trajectories generally resulted in lower values according to an SNK ($\alpha = 0.05$) test. The lowest mean value was found for case SHORT IC and was equal to 9.5. For N_8, the maximum number of aircraft pairs with less than 8-n mi separation, case FLX TMS was the only case that resulted in a higher mean score (26.1) than case CUR IDEAL (24.5); cases FLX ALT/SPD, DIRECT, and FLX LAT

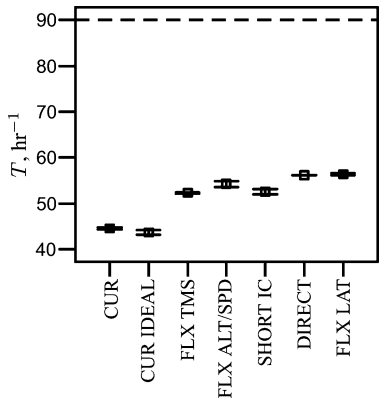

a) Throughput

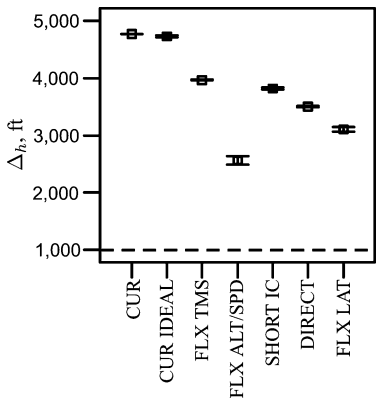

b) Deviation from continuously decreasing altitude profiles

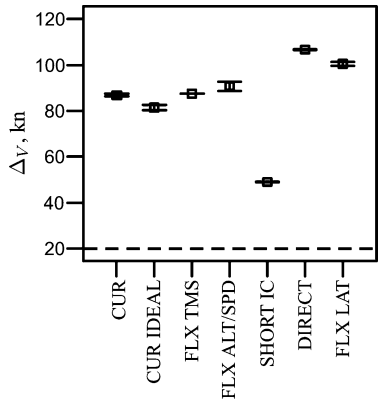

c) Deviation from continuously decreasing speed profiles

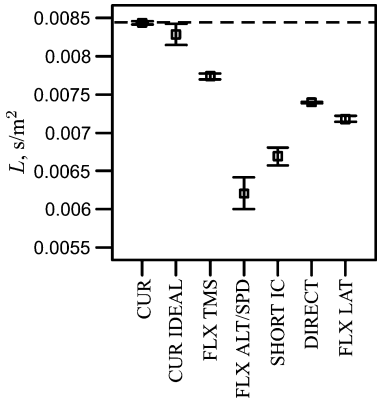

d) Noise load on community

Fig. 12 Means and 95% confidence intervals of scores on objectives.

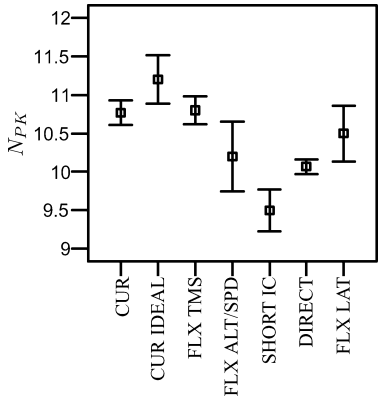

a) Peak number of aircraft

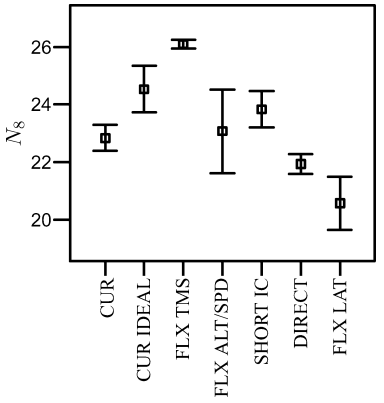

c) Maximum number of aircraft pairs with less than 8-n mi horizontal distance

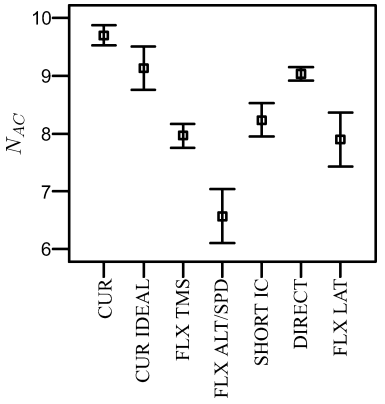

e) Maximum number of aircraft with an altitude change rate over 500 ft/min

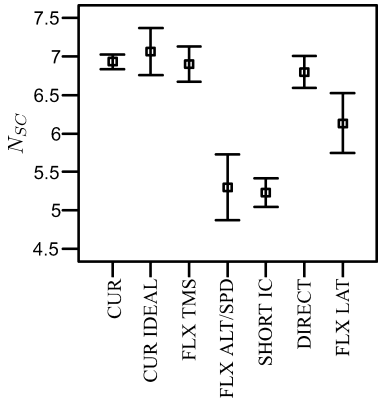

b) Maximum number of aircraft with an airspeed change greater than 10 kn during a 2-min interval

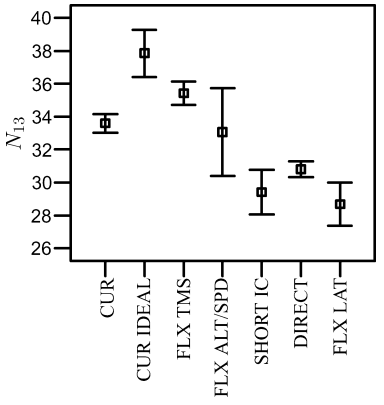

d) Maximum number of aircraft pairs with less than 13-n mi horizontal distance

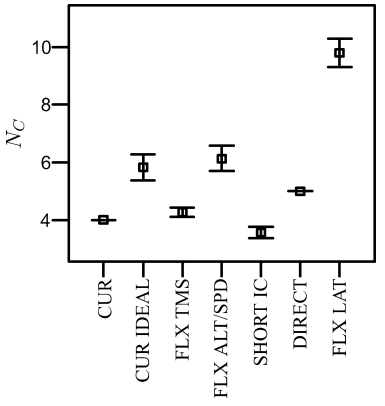

f) Number of crossing points between arrival and departure flows

Fig. 13 Means and 95% confidence intervals of airspace complexity factors 1–6.

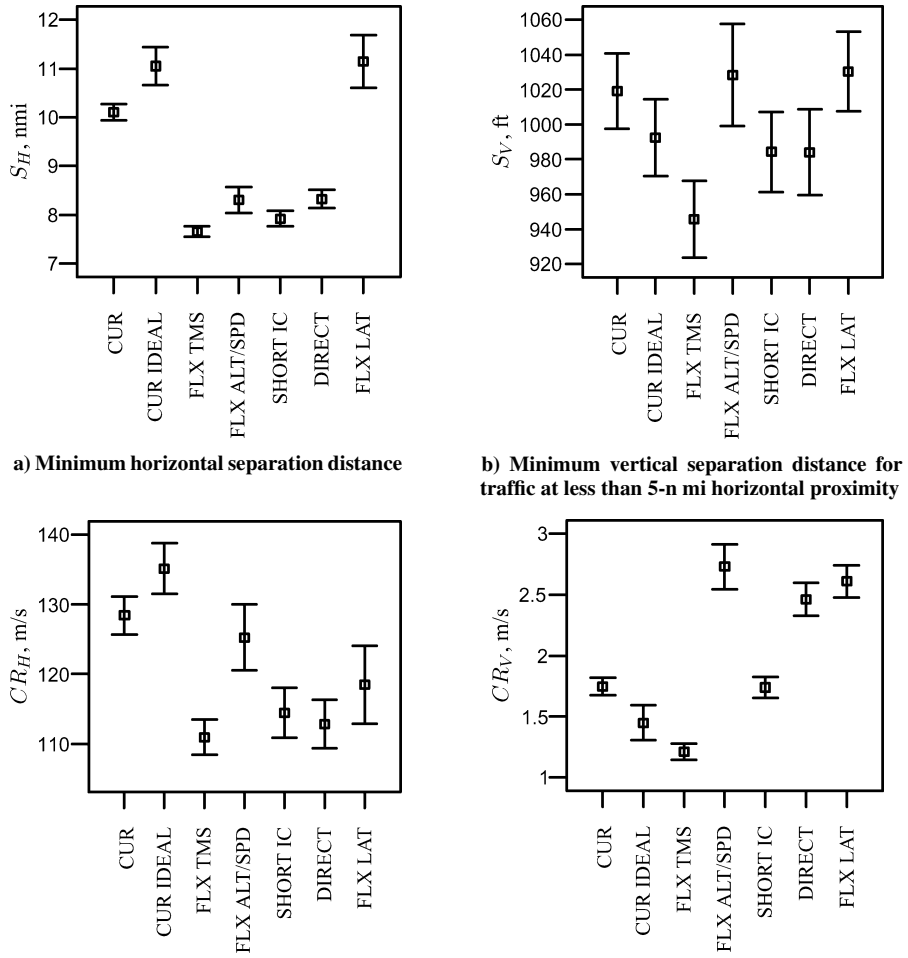

a) Minimum horizontal separation distance

b) Minimum vertical separation distance for traffic at less than 5-n mi horizontal proximity

c) Maximum horizontal closure rate

d) Maximum vertical closure rate for traffic at less than 5-n mi horizontal proximity

Fig. 14 Means and 95% confidence intervals of airspace complexity factors 7–10.

resulted in lower mean scores (23.1, 22.0, and 20.6, respectively) than case CUR IDEAL (SNK, $\alpha = 0.05$). An SNK test also showed that for the mean value of N_{13}, the maximum number of aircraft pairs with less than 13-n mi separation, flexible arrival trajectories generally resulted in lower values: For case CUR IDEAL it was 37.9, whereas the lowest value was 28.7, which was found for case FLX LAT. Based on the results for N_{pk}, N_8, and N_{13}, it can be concluded that more freedom in the trajectories helps to decrease the traffic densities and the number of aircraft at low separation distances.

For the maximum number of aircraft changing speed significantly, N_{sc}, case CUR IDEAL resulted in the highest mean value (7.1), followed by case CUR (6.9). An increasing number of aircraft simultaneously changing speed, therefore, does not seem to be a concern for the studied flexible arrival trajectories. Cases FLX ALT/SPD, SHORT IC, and FLX LAT actually decreased the mean value of N_{sc} to 5.3, 5.2, and 6.1, respectively (SNK, $\alpha = 0.05$).

A similar trend was found for the maximum number of aircraft changing altitude quickly, N_{ac}: The flexible trajectories generally resulted in lower values. The mean value was for case CUR IDEAL equal to 9.1. The lowest mean value was found for case FLX ALT/SPD and was equal to 6.6.

The mean number of crossing points, N_C, was for case CUR IDEAL equal to 5.8. It increased considerably, however, for the optimized route structure in case FLX LAT (SNK, $\alpha = 0.05$), where it was equal to 9.8. Because this value is almost two times higher than for case CUR IDEAL, an increasing number of crossing points may be an important concern for the flexible arrival trajectories.

For the horizontal separation distance S_H, the values found for case FLX LAT were comparable to those for CUR IDEAL (SNK, $\alpha = 0.05$): The mean value was equal to 11.15 n mi (20.65 km) for case FLX LAT and to 11.05 n mi (20.46 km) for case CUR IDEAL. All of the other cases resulted in statistically significant lower values than case CUR IDEAL. The lowest mean value was found for case FLX TMS, in which case it was equal to 7.66 n mi (14.19 km). Thus, all of the studied flexible arrival trajectories decreased the minimum horizontal separation as compared to the original situation, except case FLX LAT, which is due to the added horizontal flexibility that allows for more spreading of trajectories.

For the vertical separation distance S_V, the only statistically significant difference from case CUR IDEAL was found for case FLX TMS. (The mean value was 992.4 ft (302 m) for case CUR IDEAL vs 945.6 ft (288 m) for case FLX TMS, which is only a small difference.)

For the horizontal closure rate CR_H, the highest mean value was found for case CUR IDEAL (135.1 m/s). An SNK test ($\alpha = 0.05$) showed that all other cases resulted in statistically significant lower values, indicating that higher horizontal closure rates are not a concern for the flexible arrival trajectories.

For the vertical closure rate CR_V, case CUR IDEAL resulted in a mean value of 1.45 m/s. Statistically significant higher values (SNK, $\alpha = 0.05$) were found for cases FLX ALT/SPD (2.73 m/s), SHORT IC (1.74 m/s), DIRECT (2.46 m/s), and FLX LAT (2.61 m/s). It is, therefore, concluded that optimizing the altitude and speed profiles, applying a short intercept distance, applying direct routes, and optimizing the lateral profiles all can increase vertical closure rates.

Conclusions

A multi-objective scheduling algorithm was developed that provides a way to find flexible approach trajectories that meet aspiration

levels on multiple performance factors simultaneously. This was done in a sequential fashion using a genetic algorithm.

It was observed that for the currently used arrival procedures the ATM performance related to throughput, deviation from three-degree decelerated approaches, and noise impact on the community could not be increased by only optimizing runway assignments and landing times as compared to data recorded from practice. This confirms the high degree of efficiency with which the current procedures are applied.

However, changing the routes and schedules did improve the performance. It was found that changing the sequence and the times at which traffic entered the terminal area or allowing flexible arrival trajectories in the sense that the altitude and speed profiles may be optimized, that the final intercept distance may be reduced, that direct routes from the meter fix to the final intercept point are allowed, or that the lateral profiles may be optimized all resulted in more throughput, up to a maximum of 28%. In addition, applying these trajectories was shown to enable the application of altitude profiles closer to those belonging to a continuous descent approach and to allow routing flights less often over residential areas. The maximum deviation from an altitude profile belonging to a continuous descent approach was for flexible arrival trajectories up to about 2000 ft (610 m) lower than for standard arrival trajectories. The noise impact on community, modeled as a combination of time spent and altitude flown over residential areas, was reduced with up to about 25%.

A number of metrics were used to address airspace complexity. The traffic density generally became lower for flexible arrival trajectories than for conventional trajectories because more airspace could be used. The flexible trajectories could, however, result in almost doubling the number of crossing points between arrival and departure traffic, almost doubling the mean value of the maximum vertical closure rates between aircraft pairs, and reducing the mean value of the minimum horizontal separation distances between aircraft pairs with more than 3 n mi (5.56 km). Although for flexible arrival trajectories that were optimized in terms of the lateral profiles a decrease in minimum horizontal separation distance was prevented, it is concluded that flexible arrival trajectories may increase airspace complexity.

Acknowledgments

The authors wish to thank Hugo de Jonge and Bart Roeloffs from the National Aerospace Laboratory and Dries Visser from Delft University of Technology for providing valuable advice. Air Traffic Control The Netherlands is acknowledged for supplying traffic data.

References

[1]Erkelens, L. J. J., "Research into New Noise Abatement Procedures for the 21st Century," AIAA Paper 2000-4474, Aug. 2000.

[2]Clarke, J.-P. B., "Systems Analysis of Noise Abatement Procedures Enabled by Advanced Flight Guidance Technology," *Journal of Aircraft*, Vol. 37, No. 2, 2000, pp. 266–273.

[3]Clarke, J.-P. B., Ho, N. T., Ren, L., Brown, J. A., Elmer, K. R., Tong, K.-O., and Wat, J. K., "Continuous Descent Approach: Design and Flight Test for Louisville International Airport," *Journal of Aircraft*, Vol. 41, No. 5, 2004, pp. 1054–1066.

[4]Kershaw, A. D., Rhodes, D. P., and Smith, N. A., "The Influence of ATC in Approach Noise Abatement," *3rd USA/Europe Air Traffic Management Research and Development Seminar*, Paper 107, June 2000.

[5]Petre, E., "Time Based Air Traffic Control in an Extended Terminal Area: A Survey of Such Systems," *On-line Handling of Air Traffic: Management–Guidance–Control*, AGARD-AG-321, Nov. 1994, pp. 5-1–5-38.

[6]"Operational Requirements Document for EATCHIP Phase III ATM Added Functions Volume 3—Arrival Manager (CIP Advanced Level)," Eurocontrol, Rept. OPR.ET1.ST04.DEL01.3, Brussels, Jan. 1999.

[7]Prevot, T., Crane, B., Palmer, E., and Smith, N., "Efficient Arrival Management Utilizing ATC and Aircraft Automation," *Proceedings of the International Conference on Human–Computer Interaction in Aeronautics*, Cépaduès-Editions, Toulouse, 2000, pp. 183–188.

[8]Fairclough, I., "PHARE Advanced Tools Arrival Manager Final Report," Eurocontrol, Rept. DOC 98-70-18, Brussels, Aug. 1999.

[9]Vormer, F. J., Boer, E. R., van Paassen, M. M., Mulder, M., and Davison, H. J., "Constraint-Based Decision Support for Multi-Objective Arrival Traffic Planning," *Proceedings of the 22nd European Annual Conference on Human Decision Making and Control*, Univ. of Linkoping, Linkoping, Sweden, 2003, pp. 9–15.

[10]Post, W., "PHARE Demonstration 3: A Contribution to the Future of Air Traffic Management," *3rd USA/Europe Air Traffic Management Research and Development Seminar*, Paper 125, June 2000.

[11]Visser, H. G., and Wijnen, R. A. A., "Optimization of Noise Abatement Departure Trajectories," *Journal of Aircraft*, Vol. 38, No. 4, 2001, pp. 620–627.

[12]Galotti, V. P., Jr., *The Future Air Navigation System (FANS)*, Ashgate, Aldershot, Hampshire, U.K., 1997.

[13]Masalonis, A. J., Callaham, M. B., and Wanke, C. R., "Dynamic Density and Complexity Metrics for Realtime Traffic Flow Management," *5th USA/Europe Air Traffic Management Research and Development Seminar*, Paper No. 86, June 2003.

[14]Goodrich, M. A., Stirling, W. C., and Boer, E. R., "Satisficing Revisited," *Minds and Machines, Journal for Artificial Intelligence Philosophy and Cognitive Science*, Vol. 10, No. 1, 2000, pp. 79–109.

[15]Werkgroep Organisatie & Gebruik Luchtruim 2003+, "Organisatie & Gebruik Luchtruim 2003+," Luchtverkeersleiding Nederland (LVNL), Koninklijke Luchtmacht, and Nederlandse Luchtvaart Autoriteit, Hoofddorp, The Netherlands, May 2001 (in Dutch).

[16]Ruijgrok, G. J. J., *Elements of Aviation Acoustics*, Delft Univ. Press, Delft, The Netherlands, 1993, Chap. 1.

[17]Bagchi, T. P., *Multiobjective Scheduling by Genetic Algorithms*, Kluwer Academic, Norwell, MA, 1999.

[18]Zitzler, E., "Evolutionary Algorithms for Multiobjective Optimization: Methods and Applications," Ph.D. Dissertation, Computer Engineering and Networks Lab., Swiss Federal Inst. of Technology Zurich, Zurich, Nov. 1999.

[19]Ruijgrok, G. J. J., *Elements of Airplane Performance*, Delft Univ. Press, The Netherlands, Delft, 1994, Chap. 14.

[20]Gen, M., and Cheng, R., *Genetic Algorithms & Engineering Design*, Wiley, New York, 1997.

[21]Hu, X., Wu, S.-F., and Jiang, J., "GA Based On-Line Real-Time Optimization of Commercial Aircraft's Flight Path for a Free Flight Strategy," AIAA Paper 2001-4234, Aug. 2001.

[22]Gerdes, I., "Construction of Conflict-Free Routes for Aircraft in Case of Free-Routing with Genetic Algorithms," *1st USA/Europe Air Traffic Management Research and Development Seminar*, Paper No. 4, June 1997.

[23]van den Akker, J. M., van Kemenade, C. H. M., and Kok, J. N., "Evolutionary 3D-Air Traffic Flow Management," National Aerospace Lab., Rept. NLR, TP 98279, Amsterdam, June 1998.

[24]Oussedik, S., Delahaye, D., and Schoenauer, M., "Air Traffic Management by Stochastic Optimization," *2nd USA/Europe Air Traffic Management Research and Development Seminar*, Paper No. 9, Dec. 1998.

[25]Yokoyama, N., and Suzuki, S., "Modified Genetic Algorithm for Constrained Trajectory Optimization," *Journal of Guidance, Control, and Dynamics*, Vol. 28, No. 1, 2005, pp. 139–144.

[26]Hesselink, H. H., and Basjes, N., "Mantea Departure Sequencer: Increasing Airport Capacity By Planning Optimal Sequences," *2nd USA/Europe Air Traffic Management Research and Development Seminar*, Paper No. 11, Dec. 1998.

[27]Delahaye, D., Puechmorel, S., Hansman, R. J., and Histon, J. M., "Air Traffic Complexity Based on Non Linear Dynamical Systems," *5th USA/Europe Air Traffic Management Research and Development Seminar*, Paper 109, June 2003.

[28]McConnell, W. J., Jr., A Technique for Generating Arbitrarily Shaped Curved Approach Paths," NASA CR-2734, Aug. 1976.

[29]Chen, T. L., and Pritchett, A. R., "Development and Evaluation of a Cockpit Decision-Aid for Emergency Trajectory Generation," *Journal of Aircraft*, Vol. 38, No. 5, 2001, pp. 935–943.

[30]Brinton, C. R., An Implicit Enumeration Algorithm for Arrival Aircraft Scheduling," *Proceedings of the 11th Digital Avionics Systems Conference*, IEEE, New York, 1992, pp. 268–274.

[31]"User Manual for the Base of Aircraft Data (BADA)—Revision 3.3," Eurocontrol, EEC Note 20/00, Brussels, Dec. 2000.

[32]Wall, M., "GAlib: A C++ Library of Genetic Algorithm Components," Mechanical Engineering Dept., Massachusetts Inst. of Technology, Cambridge, MA, Aug. 1996.

[33]Goldberg, D. E., *Genetic Algorithms in Search, Optimization, and Machine Learning*, Addison–Wesley, Reading, MA, 1989, pp. 122–124.

[34]Vormer, F. J., "Theoretical and Operational Aspects of Optimal Airport Arrival Trajectories," Ph.D. Dissertation, Faculty of Aerospace Engineering, Delft Univ. of Technology, Delft, The Netherlands, Dec. 2005.